Journal of Metals, Materials and Minerals, Vol. 32, No. 3, pp. 86-92, 2022

Tungsten disulfide-nickel oxide hybrids as high-performance supercapacitors

Zainab Ali HRBE[1,*], and Samaher Waheed HASHIM[2]

[1] *College of Science, Wasit University, Wasit, Iraq*
[2] *Ministry of Education, General Directorate of Education Wasit, Wasit, Iraq*

***Corresponding author e-mail:** zainabali@uowasit.edu.iq

Received date:
27 July 2022
Revised date
2 August 2022
Accepted date:
2 August 2022

Keywords:
WS_2;
Supercapacitor;
Nickel oxide;
Redox

Abstract

Two-dimensional materials are suitable for energy storage applications due to their chemical stability, high electrical conductivity and large specific surface area. In this work, tungsten disulfide (WS_2) nanosheets were synthesized by chemical exfoliation method and combined with nickel oxide (NiO) nanoparticles to be used as a working electrode for storing energy. The WS_2 electrode alone shows a capacitance of about 21.87 $mF{\cdot}cm^{-2}$, which is improved up to 64.58 $mF{\cdot}cm^{-2}$ by adding NiO nanoparticles. The occurrence of redox reactions plays an important role in increasing the final capacitance. Moreover, the proposed hybrid maintains 93% of its initial capacitance after 5000 charge-discharge cycles, which indicates its stable and reliable performance.

1. Introduction

With the increase of energy consumption, the need for energy storage devices is also in high demand [1]. Among the proposed solutions, supercapacitors can be very promising as electrochemical storage devices [2,3]. These electronic devices have less capacity than batteries but deliver higher power density [4]. In addition, super-capacitor has a faster charge-discharge rate with long cycle life [5]. In order to achieve supercapacitors with high energy storage density, materials with large surface area to volume ratio, high charge transport and chemical stability are required [6]. Therefore, two-dimensional (2D) materials are attractive alternatives compared to other conventional materials [7-9]. Graphene was the first 2D material to be introduced as a supercapacitor and has shown considerable capacitance [10,11]. However, self-re-stacking of graphene sheets dramatically reduces its energy storage density which of course limits its performance [12,13]. Other 2D materials such as molybdenum disulfide (MoS_2), phosphorene etc. have been also suggested as supercapacitors, but most of them show limited capacities [14,15]. One way to improve the capacity of these materials is to combine them with other materials (such as PANI, metal oxide, etc.) to introduce a hybrid. Although PANI is conductive, it has low energy density and poor cyclic stability [16, 17]. In contrast, metal oxides play an important role in increasing hybrid capacitance by providing synergetic effects and redox reactions [18]. Up to now, supercapacitors such as PANI/graphene, MoS_2@CNT/RGO, NiO/MoS_2/rGo, NiS_2@MoS_2, and MnO_2/Graphene have been introduced that offer significant capacity compared to 2D individual electrodes[5,19-23]. Tungsten disulfide (WS_2) is another 2D material that has recently been welcomed by researchers in energy applications thanks to its layered structure which allows ions to penetrate into it leading to energy storage through the intercalation process. It also provides high capacitance through formation of a EDLC due to its high effective surface area [24]. Until now, few WS_2-based supercapacitors have been introduced, such as WO_3@WS_2, graphene@WS_2, and WS_2@α-$NiMoO_4$ [25-27]. Despite the excellent intrinsic properties of WS_2, high energy density capacitance has not been reported so far for electrodes based on it. Moreover, the fabrication of WS_2 supercapacitors has also been reported to involve complex processes that have limited its development for energy storage applications.

In this work, tungsten disulfide (WS_2) nanosheets are easily prepared by chemical sonication method and combined with nickel oxide (NiO) nanoparticles to form a supercapacitor electrode with a high capacitance performance. NiO nanoparticles are decorated on WS_2 nanosheets by depositing a 50 nm of its thin film followed by heating treatment. The fabricated electrodes are then tested in a three-electrode electrochemical cell in a 1 M Na_2SO_4 electrolyte. Based on the results, the WS_2@ NiO electrode shows a 195% increase in capacitance compared to individual WS_2 electrode, which maintains a 93% stability after 5000 charge/discharge cycles. WS_2 stores energy by providing a large surface area through electric double layer capacitance (EDLC) mechanism. Furthermore, its combination with NiO nanoparticles improves the capacitance through additional redox reactions. These two properties, together with the synergistic effects, result in the superiority of the introduced hybrid compared to individual WS_2 electrodes.

2. Experimental

2.1 Material

Tungsten disulfide powder with >99% purity was purchased from Sigma-Aldrich. N-Methyl-2-pyrrolidone (NMP) and sodium sulfate (Na_2SO_4) were supplied from Merck.

2.2 Characterization

TEM and SEM imaging were carried out by CM30m Philips and S4160 Hitachi systems, respectively. The Raman spectroscopy was done with a Renishaw Ramascope using a 532 nm laser line. XRD patterns were performed with a PANalytical X'pert Pro MPD, using Cu Kα radiation with a wavelength λ = 0.15406 nm. UV-visible spectroscopic measurement was performed by Perkin Elmer, Lambda 35. Surface morphology of electrode was characterized by NT-MDT atomic force microscopy. The thickness of the deposited NiO thin film was measured by a SENpro ellipsometer. A three-electrode electrochemical cell was used to test electrodes in a 1 M Na_2SO_4 electrolyte with Ag/AgCl reference and platinum counter electrodes. Electrochemical Impedance Spectroscopy (EIS) testing was performed by electrochemical workstation IM6 (Zahner IM6).

2.3 WS_2 nanosheets preparation

WS_2 powder (5 g) and 50 mL NMP solution was mixed and sonicated for 120 min using a probe sonicator at 300 W. Then, the obtained suspension was centrifuged at 1000 rpm for 15 min and top supernatant was collected as the final dispersion.

2.4 WS_2@NiO electrode fabrication

Two drops of WS_2 solution were cast on stainless steel substrates and dried in an oven vacuum at 70°C. Then, 50 nm of nickel oxide film was sputtered on samples and annealed at 300°C under argon atmosphere for 30 min. Next, electrodes were soldered with silver paste and all opening except the surface of the samples were passivated with epoxy glue.

3. Results and discussion

Figure 1(a) exhibits a scanning electron microscopy (SEM) of WS_2 nanosheets. The nanosheets are evenly coated on the substrate and provide a large surface area to volume ratio for supercapacitor applications. Figure 1b presents a transmission electron microscope (TEM) image of WS_2 nanosheets on a carbon grid. The transparency of the layers indicates their nanometer thicknesses. The thickness of one part of the deposited film on the substrate is shown in Figure 1(c) by atomic force microscopy (AFM) analysis. In 30 μm^2 × 30 μm^2 window, a maximum thickness of 150 nm is measured for the nanosheets, which indicates the coverage of the substrate with nanometric thicknesses.

One of the analysis that is suitable for characterizing 2D materials is Raman measurement. In this analysis, each 2D material has its own characteristic peaks that their location in the bulk mode can be different from the multilayer mode [28]. In the case of WS_2, Raman test is performed for both bulk and nanosheets cases. Figure 2(a) shows the Raman spectra of the bulk WS_2 and its nanosheets. WS_2 has two oscillation modes, one of which is caused by an in-plane phonon oscillation called E^1_{2g}, and the other of an out-of-plane phonon oscillation called A_{1g} [29]. In the bulk state, the position of the E^1_{2g} and A_{1g} peaks are measured at 351 and 420 cm^{-1}, respectively. For WS_2 nanosheets, the locations of these peaks are shifted to 354 and 416 cm^{-1}, indicating their lower thickness in respect to of the bulk WS_2. Schematics of the atom oscillations of both modes are also drawn inside the Figure 2(a). Figure 2(b) demonstrates the absorption spectrum of the WS_2 dispersion which contains three peaks of C, B, and A at 470, 521, and 632 nm, respectively [30]. The peaks A and B are due to the exciton transitions at the k point, while peak C is due to the exciton transitions at the Γ point of the Brillouin zones [30]. The presence of all three peaks strongly indicates the presence of WS_2 nanosheets in the prepared dispersion.

After synthesizing WS_2 nanosheets, they are deposited on a stainless steel substrate and 50 nm of nickel oxide is sputtered on it. The layer thickness is controlled by the ellipsometry measurement. The sample is then heated at 300°C in argon atmosphere for 30 min to convert the layer into nickel oxide nanoparticles. The schematic illustration of the fabrication steps of the electrodes is presented in Figure 3. Accordingly, WS_2 nanosheets were deposited on the stainless steel substrate followed by sputtering 50 nm NiO film. Then, the sample was heated up at 300°C under argon atmosphere for 30 min. Finally, the electrodes were soldered and passivated in order to use in the electrochemical cell.

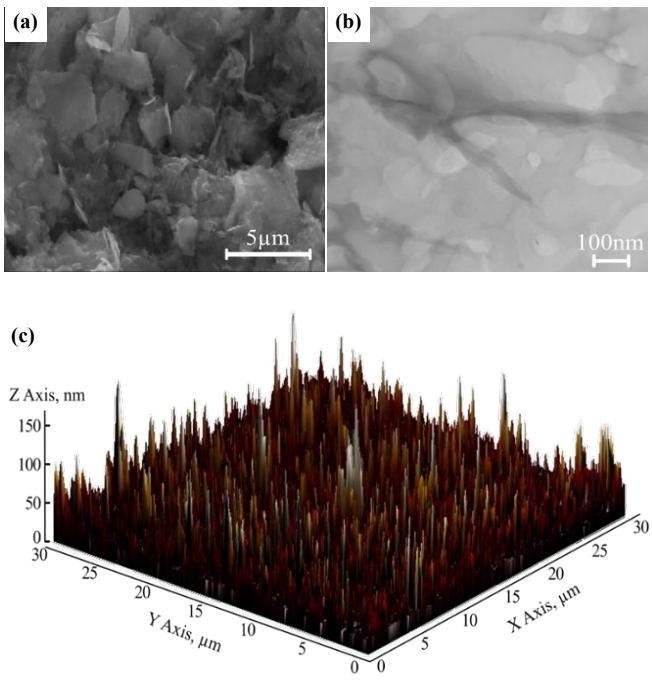

Figure 1. *(a)* Scanning electron microscopy image of the WS_2 nanosheets on the substrate, (b) Transmission electron microscope image of WS_2 nanosheets on the carbon grid, and (c) Atomic force microscopy analysis of the WS_2 nanosheets on the 30 μm^2 × 30 μm^2 window of the substrate with the corresponding z values.

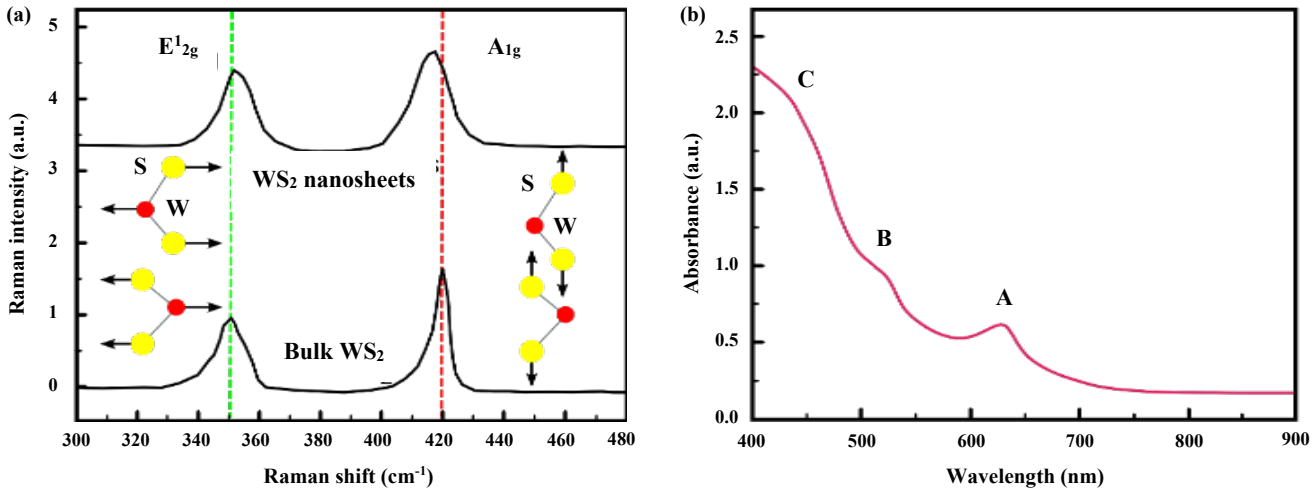

Figure 2. (a) Raman spectra of the WS_2 in both bulk and nanosheets form, and (b) Absorption spectrum of the WS_2 dispersion with corresponding A, B, and C peaks.

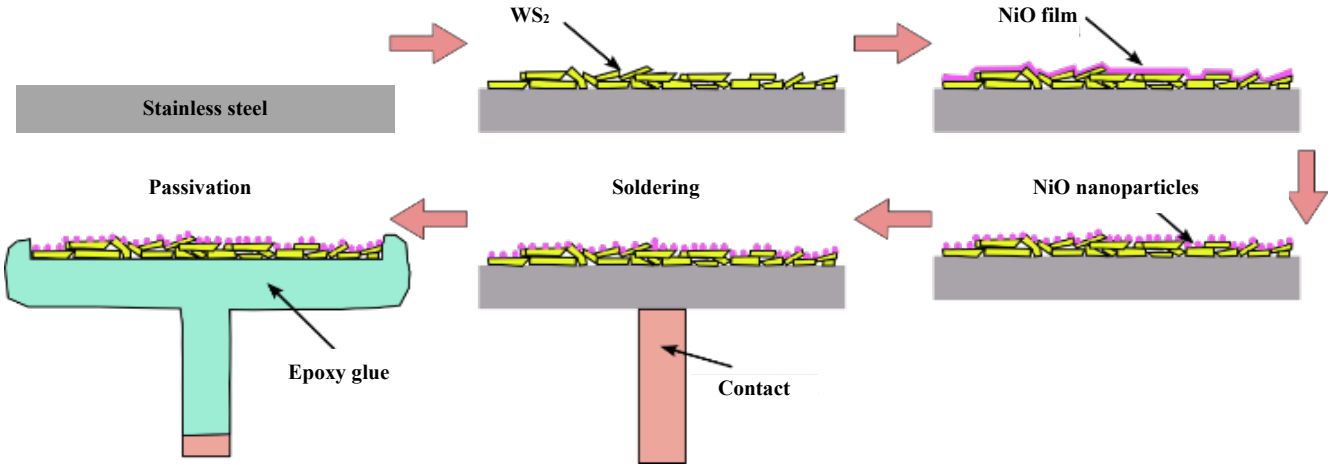

Figure 3. Schematic illustration of the electrode fabrication process.

Figure 4(a) exhibits the SEM image of nanoparticles on the substrate. The approximate diameters of the nanoparticles are measured at about 100 nm. Figure 4(b) shows the SEM image of the nanoparticles on a WS_2 nanosheet where the NiO nanoparticles cover the entire surface of the WS_2 nanosheets.

Figure 5 shows the XRD spectra of NiO, WS_2 nanosheets and WS_2@NiO hybrids. In the case of WS_2, (002), (004), (100), (101), (103), (006), (105), (110), (008), and (112) peaks are located at 14.11°, 28.06°, 33.02°, 33.84°, 39.43°, 44.27°, 50.01°, 58.30°, 60.10°, and 61.15°, respectively [31]. In the XRD spectrum of the NiO sample, (111), (200), (220), (311), and (222) peaks are placed at 36.76°, 42.11°, 61.42°, 74.35°, and 78.11°, respectively [32]. Accordingly, diffraction peaks of both structures are observable in the hybrid sample, which confirms its successful synthesis.

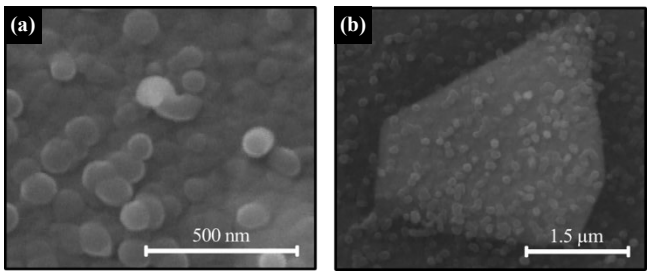

Figure 4. SEM image of (a) NiO nanoparticles with approximate diameter of 100 nm, and (b) WS_2 nanosheet decorated with NiO nanoparticle.

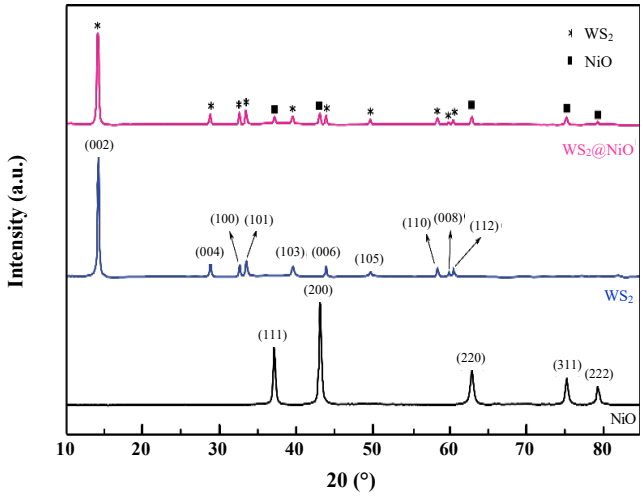

Figure 5. XRD pattern of NiO, WS_2, and WS_2@NiO samples.

The fabricated electrodes are used as working electrodes in a three-electrode electrochemical cell. 1 M Na_2SO_4 solution is used as electrolyte. Figure 6(a) shows the current-voltage test of the WS_2 electrode. It can be seen that the curves have a rectangular shape, which is mainly due to the EDLC behavior of WS_2 nanosheets. Although the internal area of the curves increases as the scan rate increases, the final capacitance decreases [5]. According to the results, the capacitance of 21.87, 13.33, 11.66, 10.41 and 6.14 $mF{\cdot}cm^{-2}$ are calculated for 5 $mV{\cdot}s^{-1}$ to 200 $mV{\cdot}s^{-1}$ scan rates, respectively. Figure 6(b) presents the current-voltage test of a WS_2@NiO electrode that was performed similar to the previous test. Unlike WS_2 electrode, redox peaks are observed here, which may be due to the presence of NiO nanoparticles. For this electrode, capacitance value of 64.58, 28.33, 24.16, 17.91 and 13.12 $mF{\cdot}cm^{-2}$ are calculated at scan rates of 5 $mV{\cdot}s^{-1}$ to 200 $mV{\cdot}s^{-1}$, respectively. Figure 6(c) compares the calculated capacitance of both electrodes in respect to different scan rates. Accordingly, the WS_2@NiO electrode delivers more capacitance values at all scan rates compared with WS_2 electrode, which can be due to the redox reactions and synergistic effects of NiO nanoparticles with WS_2 nanosheets [33]. Table 1 shows the calculated capacitance values of both electrodes.

Figure 6(d) displays the charge-discharge test of both electrodes under a constant current density of 0.35 $mA{\cdot}cm^{-2}$ in a 600 mV voltage window. The charge-discharge curve of the WS_2 electrode is perfectly symmetric, which is consistent with the results of its voltammetric test, while for the WS_2@NiO electrode asymmetry is observed due to the redox reactions [28,34]. However, it is observed that the discharge time of the hybrid electrode is longer than the WS_2 electrode.

Table 1. Capacitance value of WS_2 and WS_2@NiO electrodes at different scan rates of 5, 25, 50, 100, and 200 $mV{\cdot}s^{-1}$.

Scan rate ($mV{\cdot}s^{-1}$)	Capacitance ($mF{\cdot}cm^{-2}$)	
	WS_2	WS_2@NiO
5	21.87	64.58
25	13.33	28.33
50	11.66	24.16
100	10.41	17.91
200	6.14	13.12

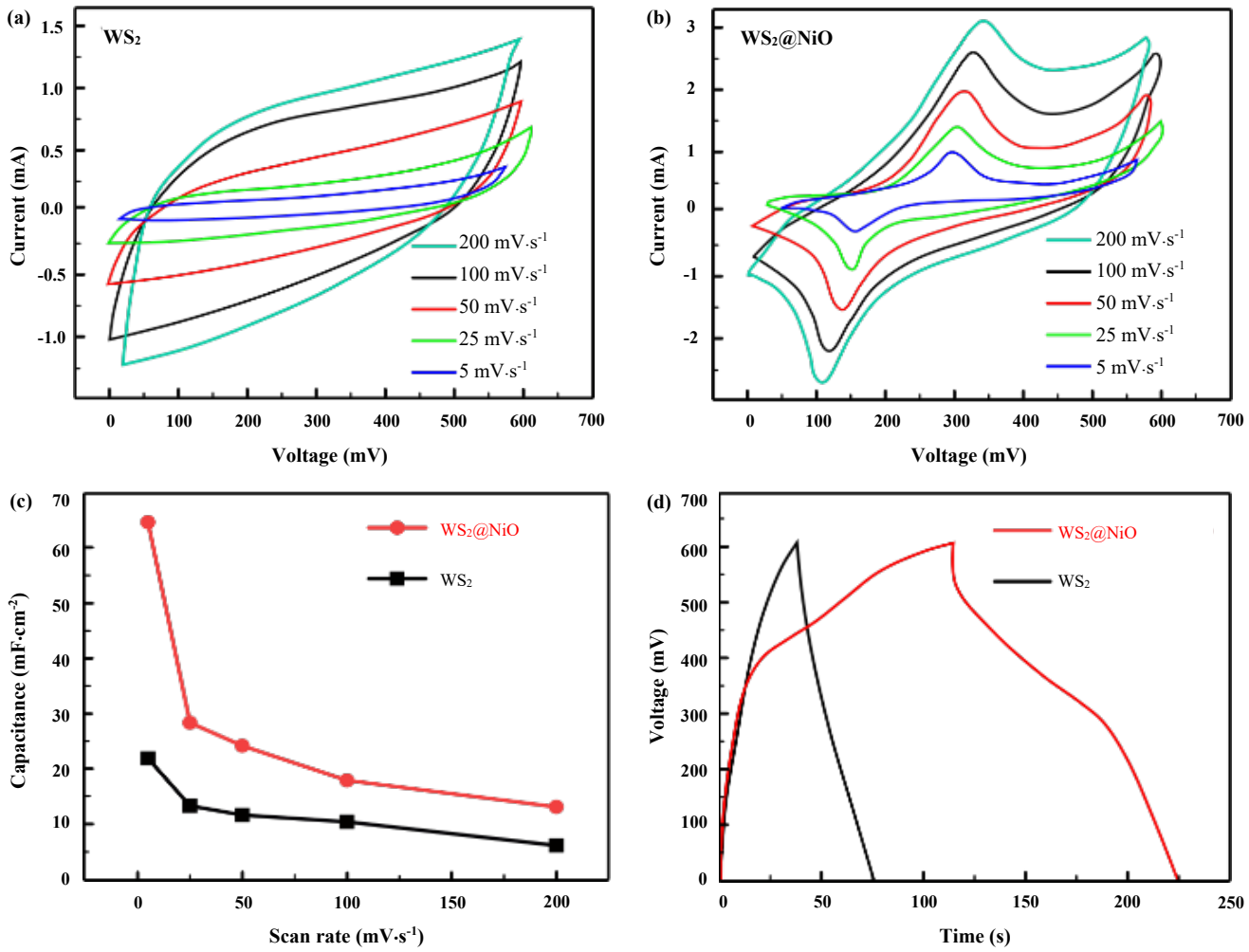

Figure 6. Voltammetry test of the (a) WS_2, (b) WS_2@NiO electrodes at different scan rates, (c) Capacitance values of the electrodes as a function of scan rates, and (d) Charge-discharge test of the electrodes at a constant current density of 0.35 $mA{\cdot}cm^{-2}$.

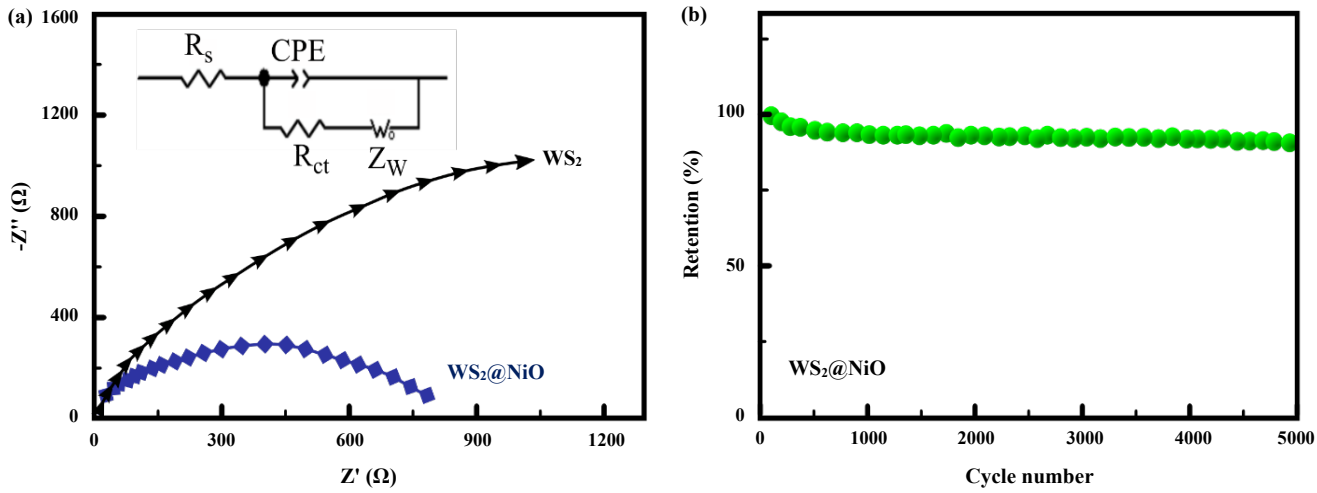

Figure 7. EIS spectra of the WS_2, and WS_2@NiO electrodes. (a) Inset shows the equivalent circuit of the electrode, and (b) Capacitance retention test of the WS_2@NiO electrode for 5000 charge-discharge cycles.

Table 2. Comparison of capacitive performance of WS_2 based supercapacitors.

Electrode Material	Electrolyte	Scan rate	Specific capacitance	ref
WS_2 nanosheets	PVA-H_3PO_4	100 mV·s^{-1}	13.0 mF·cm^{-2}	[35]
WS_2 QDs	PVA-H_3PO_4	100 mV·s^{-1}	22.0 mF·cm^{-2}	[35]
WO_3@WS_2	0.1 M Na_2SO_4	5 mV·s^{-1}	47.5 mF·cm^{-2}	[36]
WS_2/PEDOT:PSS	1 M H_2SO_4	40 mV·s^{-1}	86.0 mF·cm^{-2}	[37]
WS_2/PANI	1 M Na_2SO_4	100 mV·s^{-1}	4.0 mF·cm^{-2}	[38]
WS_2@NiO	1 M Na_2SO_4	5 mV·s^{-1}	64.5 mF·cm^{-2}	This work

Electrochemical Impedance Spectroscopy (EIS) analysis is performed to compare the performance of the two electrodes in energy storage. The EIS spectrum of two electrodes are shown in Figure 7(a), where the WS_2@NiO electrode reveals a smaller radius than the WS_2 electrode. This behavior may be due to lower internal resistance in the former sample, which allows ion transport to be carried out more efficiently [28]. Inset of Figure 7(a) also shows the equivalent circuit of the electrodes. Moreover, after 5000 charge-discharge cycles testing of WS_2@NiO electrode, it retained 93% of its initial capacitance as shown in Figure 7(b). The high cyclic stability of the WS_2@NiO electrode along with its high capacitance value indicates its excellent potential that can be developed as a commercial supercapacitor

According to CV curves, the predominant energy storage mechanism in WS_2 nanosheets is EDCL behavior, while in NiO nanoparticles it shows pseudocapacitance behavior due to redox peaks. As a result, the energy storage process can be described in the hybrid as follows [5]:

$$(MoS_2)_{surface} + Na^+ + e^- \leftrightarrow (MoS_2^- - Na^+)_{surface} \quad (1)$$

$$NiO + Na^+ + e^- \leftrightarrow (NiO - Na^+)_{surface} \quad (2)$$

Table 2 compares the performance of the previously reported electrodes with our introduced WS_2@NiO hybrid. Accordingly, WS_2@NiO hybrid shows considerable capacitive properties compared with other electrodes.

4. Conclusions

Two-dimensional materials are suitable for energy storage applications due to their large surface area. However, experimental results show that these materials deliver limited capacitance. In this work, WS_2 nanosheets were easily synthesized by chemical sonication and combined with NiO nanoparticles to be used as electrodes for supercapacitor applications. The results showed that the WS_2@NiO electrode stored 195% more energy than the WS_2 electrode with retaining 93% of its initial capacitance even after 5000 charge-discharge cycles. The extraordinary performance of this electrode can introduce it as a commercial supercapacitor.

References

[1] N. Namdar, F. Ghasemi, and Z. Sanaee, "Plasma-assisted three-dimensional lightscribe graphene as high-performance super-capacitors," *Scientific Reports,* vol. 12, p. 4254, 2022.

[2] W. Raza, F. Ali, N. Raza, Y. Luo, K.-H. Kim, J. Yang, S. Kumar, A. Mehood, and E. E. Kwon, "Recent advancements in super-capacitor technology," *Nano Energy,* vol. 52, pp. 441-473, 2018.

[3] K. Songmueang, D. Zhang, J. Cao, X. Zhang, S. Kheawhom, C. Sriprachuabwong, A. Tuantranont, P. Wangyao, and J. Qin, "Flower-like W/WO_3 as a novel cathode for aqueous zinc-ion batteries," *Chemical Communications,* vol. 57, pp. 7549-7552, 2021.

[4] J. Li, N. Wang, J. Tian, W. Qian, and W. Chu, "Cross-coupled macro-mesoporous carbon network toward record high energy-power density supercapacitor at 4 V," *Advanced Functional Materials,* vol. 28, p. 1806153, 2018.

[5] F. Ghasemi, M. Jalali, A. Abdollahi, S. Mohammadi, Z. Sanaee, and S. Mohajerzadeh, "A high performance supercapacitor based on decoration of MoS_2/reduced graphene oxide with NiO nanoparticles," *RSC Advances,* vol. 7, pp. 52772-52781, 2017.

[6] H. Li, R. Chen, M. Ali, H. Lee, and M. J. Ko, "In situ grown MWCNTs/MXenes nanocomposites on carbon cloth for high-performance flexible supercapacitors," *Advanced Functional Materials,* vol. 30, p. 2002739, 2020.

[7] S. G. Krishnan, A. Arunachalam, P. Jagadish, and M. Khalid, "2D Materials for supercapacitor and supercapattery applications," in *Adapting 2D Nanomaterials for Advanced Applications*. vol. 1353, ed: American Chemical Society, 2020, pp. 33-47.

[8] F. Ghasemi, "Vertically aligned carbon nanotubes, MoS_2–rGo based optoelectronic hybrids for NO2 gas sensing," *Scientific Reports,* vol. 10, p. 11306, 2020.

[9] J. Cao, D. Zhang, R. Chanajaree, Y. Yue, Z. Zeng, X. Zhang, and J. Qin, "Stabilizing zinc anode via a chelation and desolvation electrolyte additive," *Advanced Powder Materials,* vol. 1, p. 100007, 2022.

[10] M. H. Amiri, N. Namdar, A. Mashayekhi, F. Ghasemi, Z. Sanaee, and S. Mohajerzadeh, "Flexible micro supercapacitors based on laser-scribed graphene/ZnO nanocomposite," *Journal of Nanoparticle Research,* vol. 18, p. 237, 2016.

[11] Y. Wang, Z. Shi, Y. Huang, Y. Ma, C. Wang, M. Chen, and Y. Chen, "Supercapacitor devices based on graphene materials," *The Journal of Physical Chemistry C,* vol. 113, pp. 13103-13107, 2009.

[12] V. D. Nithya, "A review on holey graphene electrode for supercapacitor," *Journal of Energy Storage,* vol. 44, p. 103380, 2021.

[13] J. Cao, D. Zhang, Y. Yue, X. Wang, A. Srikhaow, C. Sriprachuabwong, A. Tuantranont, X. Zhang, Z-S. Wu, and J. Qin, "Strongly coupled tungsten oxide/carbide heterogeneous hybrid for ultrastable aqueous rocking-chair zinc-ion batteries," *Chemical Engineering Journal,* vol. 426, p. 131893, 2021.

[14] H. Tang, J. Wang, H. Yin, H. Zhao, D. Wang, and Z. Tang, "Growth of polypyrrole ultrathin films on mos2 monolayers as high-performance supercapacitor electrodes," *Advanced Materials,* vol. 27, pp. 1117-1123, 2015.

[15] L. Zu, X. Gao, H. Lian, C. Li, Q. Liang, Y. Liang, X. Cui, Y. Liu, X. Wang, and X. Cui, "Electrochemical prepared phosphorene as a cathode for supercapacitors," *Journal of Alloys and Compounds,* vol. 770, pp. 26-34, 2019.

[16] Q. Chen, F. Xie, G. Wang, K. Ge, H. Ren, M. Yan, Q. Wang, and H. Bi, "Hybrid MoS_2@PANI materials for high-performance supercapacitor electrode," *Ionics,* vol. 27, pp. 4083-4096, 2021.

[17] J. Abdulla, J. Cao, P. Wangyao, and J. Qin, "Review on the suppression of Zn dendrite for high performance of Zn ion battery," *Journal of Metals, Materials and Minerals,* vol. 30, 2020.

[18] N. Shaheen, M. Aadil, S. Zulfiqar, H. Sabeeh, P. O. Agboola, M. F. Warsi, M. F. Aly Aboud, and I. Shakir, "Fabrication of different conductive matrix supported binary metal oxides for supercapacitors applications," *Ceramics International,* vol. 47, pp. 5273-5285, 2021.

[19] N. Chen, L. Ni, J. Zhou, G. Zhu, Q. Kang, Y. Zhang, S. Chen, W. Zhou, C. Lu, J. Chen, X. Feng, X. Wang, X. Guo, L. Peng, W. Ding, and W. Hou, "Sandwich-Like holey graphene/pani/graphene nanohybrid for ultrahigh-rate supercapacitor," *ACS Applied Energy Materials,* vol. 1, pp. 5189-5197, 2018.

[20] S. Hou, Y. Lian, Z. Xu, D. Wang, C. Ban, J. Zhao, and H. Zhang, "Construction of ball-flower like NiS_2@MoS_2 composite for high performance supercapacitors," *Electrochimica Acta,* vol. 330, p. 135208, 2020.

[21] L. Peng, X. Peng, B. Liu, C. Wu, Y. Xie, and G. Yu, "Ultrathin Two-dimensional MnO_2/graphene hybrid nanostructures for high-performance, flexible planar supercapacitors," *Nano Letters,* vol. 13, pp. 2151-2157, 2013.

[22] S. Wang, J. Zhu, Y. Shao, W. Li, Y. Wu, L. Zhang, and X. Hau, "Three-dimensional MoS_2@CNT/RGO network composites for high-performance flexible supercapacitors," *Chemistry – A European Journal,* vol. 23, pp. 3438-3446, 2017.

[23] N. Keawploy, R. Venkatkarthick, P. Wangyao, and J. Qin, "Screen printed textile electrodes using graphene and carbon nanotubes with silver for flexible supercapacitor applications," *Journal of Metals, Materials and Minerals,* vol. 30, pp. 39-44, 2020.

[24] J. Jiang, Y. Zhang, P. Nie, G. Xu, M. Shi, J. Wang, Y. Wu, R. Fu, H. Dou, and X. Zhang, "Progress of nanostructured electrode materials for supercapacitors," *Advanced Sustainable Systems,* vol. 2, p. 1700110, 2018.

[25] W. Chen, X. Yu, Z. Zhao, S. Ji, and L. Feng, "Hierarchical architecture of coupling graphene and 2D WS_2 for high-performance supercapacitor," *Electrochimica Acta,* vol. 298, pp. 313-320, 2019.

[26] K. S. Kumar, N. Choudhary, D. Pandey, L. Hurtado, H.-S. Chung, L. Tetard, Y. Jung, and J. Tomas, "High-performance flexible asymmetric supercapacitor based on rGO anode and WO_3/WS_2 core/shell nanowire cathode," *Nanotechnology,* vol. 31, p. 435405, 2020.

[27] S. K. Ray, B. Pant, M. Park, J. Hur, and S. W. Lee, "Cavity-like hierarchical architecture of WS_2/α-$NiMoO_4$ electrodes for supercapacitor application," *Ceramics International,* vol. 46, pp. 19022-19027, 2020.

[28] F. Ghasemi, and M. Hassanpour Amiri, "Facile in situ fabrication of rGO/MoS_2 heterostructure decorated with gold nanoparticles with enhanced photoelectrochemical performance," *Applied Surface Science,* vol. 570, p. 151228, 2021.

[29] S. Sinha, S. Kumar, S. K. Arora, A. Sharma, M. Tomar, H.-C. Wu, and W. Gupta, "Enhanced interlayer coupling and efficient photodetection response of in-situ grown MoS_2–WS_2 van der waals heterostructures," *Journal of Applied Physics,* vol. 129, p. 155304, 2021.

[30] E. Rahmanian, and R. Malekfar, "Size-dependent optical response of few-layered WS_2 nanosheets produced by liquid phase

exfoliation," *The European Physical Journal Applied Physics,* vol. 77, p. 30401, 2017.

[31] J.-P. Zou, J. Ma, J.-M. Luo, J. Yu, J. He, Y. Meng, Z. Luo, S-K. Bao, H-L. Liu, S-L. Luo, X-B. Luo, T-C. Chen, and S. L. Siib, "Fabrication of novel heterostructured few layered WS_2-Bi_2WO_6/$Bi_{3.84}W_{0.16O6.24}$ composites with enhanced photo-catalytic performance," *Applied Catalysis B: Environmental,* vol. 179, pp. 220-228, 2015.

[32] Z. Sabouri, N. Fereydouni, A. Akbari, H. A. Hosseini, A. Hashemzadeh, M. S. Amiri, R. K. Oskuee, and M. Darroudi, "Plant-based synthesis of NiO nanoparticles using salvia macrosiphon boiss extract and examination of their water treatment," *Rare Metals,* vol. 39, pp. 1134-1144, 2020.

[33] S. Chandra Sekhar, J.-H. Lee, E.-B. Cho, and J. S. Yu, "Unveiling redox-boosted mesoporous Co@NiO–SiO_2 hybrid composite with hetero-morphologies as an electrode candidate for durable hybrid supercapacitors," *Journal of Materials Research and Technology,* vol. 13, pp. 1899-1907, 2021.

[34] A. Abdollahi, A. Abnavi, F. Ghasemi, S. Ghasemi, Z. Sanaee, and S. Mohajerzadeh, "Facile synthesis and simulation of MnO_2 nanoflakes on vertically aligned carbon nanotubes, as a high-performance electrode for Li-ion battery and supercapacitor," *Electrochimica Acta,* vol. 390, p. 138826, 2021.

[35] A. Ghorai, A. Midya, and S. K. Ray, "Superior charge storage performance of WS_2 quantum dots in a flexible solid state supercapacitor," *New Journal of Chemistry,* vol. 42, pp. 3609-3613, 2018.

[36] N. Choudhary, C. Li, H.-S. Chung, J. Moore, J. Thomas, and Y. Jung, "High-performance one-body core/shell nanowire supercapacitor enabled by conformal growth of capacitive 2D WS_2 layers," *ACS Nano,* vol. 10, pp. 10726-10735, 2016.

[37] A. Liang, D. Li, W. Zhou, Y. Wu, G. Ye, J. Wu, Y. Chang, R. Wang, J. Xu, G. Nie, J. Hou, and Y. Du, "Robust flexible WS_2/PEDOT:PSS film for use in high-performance miniature supercapacitors," *Journal of Electroanalytical Chemistry,* vol. 824, pp. 136-146, 2018.

[38] A. De Adhikari, N. Shauloff, Y. Turkulets, I. Shalish, and R. Jelinek, "Tungsten-disulfide/polyaniline high frequency supercapacitors," *Advanced Electronic Materials,* vol. 7, p. 2100025, 2021.